

# Self-mode-locking semiconductor disk laser

Mahmoud Gaafar,<sup>1,\*</sup> Philipp Richter,<sup>1</sup> Hakan Keskin,<sup>2</sup> Christoph Möller,<sup>1</sup>  
Matthias Wichmann,<sup>1</sup> Wolfgang Stolz,<sup>1,3</sup> Arash Rahimi-Iman,<sup>1</sup> and Martin Koch<sup>1</sup>

<sup>1</sup>Department of Physics and Materials Sciences Center, Philipps-Universität Marburg, Renthof 5, 35032 Marburg, Germany

<sup>2</sup>Department of Physics, Middle East Technical University, Ankara, 06800, Turkey

<sup>3</sup>NAsP III/V GmbH, Am Knechtacker 19, 35041 Marburg, Germany

\*mahmoud.gaafar@physik.uni-marburg.de

**Abstract:** The development of mode-locked semiconductor disk lasers received striking attention in the last 14 years and there is still a vast potential of such pulsed lasers to be explored and exploited. While for more than one decade pulsed operation was strongly linked to the employment of a saturable absorber, self-mode-locking emerged recently as an effective and novel technique in this field – giving prospect to a reduced complexity and improved cost-efficiency of such lasers. In this work, we highlight recent achievements regarding self-mode-locked semiconductor devices. It is worth to note, that although nonlinear effects in the active medium are expected to give rise to self-mode-locking, this has to be investigated with care in future experiments. However, there is a controversy whether results presented with respect to self-mode-locking truly show mode-locking. Such concerns are addressed in this work and we provide a clear evidence of mode-locking in a saturable-absorber-free device. By using a BBO crystal outside the cavity, green light originating from second-harmonic generation using the out-coupled laser beam is demonstrated. In addition, long-time-span pulse trains as well as radiofrequency-spectra measurements are presented for our sub-ps pulses at 500 MHz repetition rate which indicate the stable pulse operation of our device. Furthermore, a long-time-span autocorrelation trace is introduced which clearly shows absence of a pedestal or double pulses. Eventually, a beam-profile measurement reveals the excellent beam quality of our device with an M-square factor of less than 1.1 for both axes, showing that self-mode-locking can be achieved for the fundamental transverse mode.

©2014 Optical Society of America

**OCIS codes:** (140.4050) Mode-locked lasers; (140.5960) Semiconductor lasers; (140.7270) Vertical emitting lasers.

---

## References and links

1. M. Kuznetsov, F. Hakimi, R. Sprague, and A. Mooradian, “High-power (>0.5-W CW) diode-pumped vertical-external-cavity surface-emitting semiconductor lasers with circular TEM<sub>00</sub> beams,” *IEEE Photon. Technol. Lett.* **9**(8), 1063–1065 (1997).
2. B. Heinen, T. L. Wang, M. Sparenberg, A. Weber, B. Kunert, J. Hader, S. W. Koch, J. V. Moloney, M. Koch, and W. Stolz, “106 W continuous-wave output power from vertical-external-cavity surface-emitting laser,” *Electron. Lett.* **48**(9), 516–517 (2012).
3. F. Zhang, B. Heinen, M. Wichmann, C. Möller, B. Kunert, A. Rahimi-Iman, W. Stolz, and M. Koch, “A 23-watt single-frequency vertical-external-cavity surface-emitting laser,” *Opt. Express* **22**(11), 12817–12822 (2014).
4. M. Wichmann, M. K. Shakfa, F. Zhang, B. Heinen, M. Scheller, A. Rahimi-Iman, W. Stolz, J. V. Moloney, S. W. Koch, and M. Koch, “Evolution of multi-mode operation in vertical-external-cavity surface-emitting lasers,” *Opt. Express* **21**(26), 31940–31950 (2013).
5. U. Keller and A. C. Tropper, “Passively modelocked surface-emitting semiconductor lasers,” *Phys. Rep.* **429**(2), 67–120 (2006).
6. T. Schwarzbäck, H. Kahle, M. Eichfelder, R. Roßbach, M. Jetter, and P. Michler, “Wavelength tunable ultraviolet laser emission via intra-cavity frequency doubling of an AlGaInP vertical external-cavity surface-emitting laser down to 328 nm,” *Appl. Phys. Lett.* **99**(26), 261101 (2011).

7. M. Scheller, J. M. Yarborough, J. V. Moloney, M. Fallahi, M. Koch, and S. W. Koch, "Room temperature continuous wave milliwatt terahertz source," *Opt. Express* **18**(26), 27112–27117 (2010).
8. M. Wichmann, M. Stein, A. Rahimi-Iman, S. W. Koch, and M. Koch, "Interferometric Characterization of a Semiconductor Disk Laser driven Terahertz Source," *J. Infrared Milli. Terahz. Waves* **35**(6-7), 503–508 (2014).
9. S. Hoogland, S. Dhanjal, A. C. Tropper, S. J. Roberts, R. Häring, R. Paschotta, and U. Keller, "Passively mode-locked diode-pumped surface-emitting semiconductor laser," *IEEE Photon. Technol. Lett.* **12**(9), 1135–1137 (2000).
10. R. Häring, R. Paschotta, E. Gini, F. Morier-Genoud, D. Martin, H. Melchior, and U. Keller, "Picosecond surface-emitting semiconductor laser with > 200 mW average power," *Electron. Lett.* **37**(12), 766–767 (2001).
11. A. Gamache, S. Hoogland, A. Trooper, I. Sagnes, G. Saint-Girons, and J. S. Roberts, "Sub-500-fs soliton-like pulse in a passively mode-locked broadband surface-emitting laser with 100 mW average power," *Appl. Phys. Lett.* **80**(21), 3892–3894 (2002).
12. R. Häring, R. Paschotta, A. Aschwanden, E. Gini, F. Morier-Genoud, and U. Keller, "High-power passively mode-locked semiconductor lasers," *IEEE J. Quantum Electron.* **38**(9), 1268–1275 (2002).
13. D. Lorensen, H. J. Unold, D. J. H. C. Maas, A. Aschwanden, R. Grange, R. Paschotta, D. Ebling, E. Gini, and U. Keller, "Towards wafer-scale integration of high repetition rate passively mode-locked surface-emitting semiconductor lasers," *Appl. Phys. B* **79**(8), 927–932 (2004).
14. S. Hoogland, A. Gamache, I. Sagnes, J. S. Roberts, and A. C. Tropper, "10-GHz train of sub-500-fs optical soliton-like pulses from a surface-emitting semiconductor laser," *IEEE Photon. Technol. Lett.* **17**(2), 267–269 (2005).
15. O. Casel, D. Woll, M. A. Tremont, H. Fuchs, R. Wallenstein, E. Gerster, P. Unger, M. Zorn, and M. Weyers, "Blue 489-nm picosecond pulses generated by intracavity frequency doubling in a passively mode-locked optically pumped semiconductor disk laser," *Appl. Phys. B* **81**(4), 443–446 (2005).
16. D. Lorensen, D. J. H. C. Maas, H. J. Unold, A. R. Bellancourt, B. Rudin, E. Gini, D. Ebling, and U. Keller, "50-GHz passively mode-locked surface-emitting semiconductor laser with 100-mW average output power," *IEEE J. Quantum Electron.* **42**(8), 838–847 (2006).
17. E. J. Saarinen, A. Härkönen, R. Herda, S. Suomalainen, L. Orsila, T. Hakulinen, M. Guina, and O. G. Okhotnikov, "Harmonically mode-locked VECSELs for multi-GHz pulse train generation," *Opt. Express* **15**(3), 955–964 (2007).
18. M. Hoffmann, Y. Barbarin, D. Maas, M. Golling, I. L. Krestnikov, S. S. Mikhlin, A. R. Kovsh, T. Südmeyer, and U. Keller, "Modelocked quantum dot vertical external cavity surface emitting laser," *Appl. Phys. B* **93**(4), 733–736 (2008).
19. K. G. Wilcox, M. Butkus, I. Farrer, D. A. Ritchie, A. Tropper, and E. U. Rafailov, "Subpicosecond quantum dot saturable absorber mode-locked semiconductor disk laser," *Appl. Phys. Lett.* **94**(25), 251105 (2009).
20. K. G. Wilcox, A. H. Quarterman, H. Beere, D. A. Ritchie, and A. C. Tropper, "High Peak Power Femtosecond Pulse Passively Mode-Locked Vertical-External-Cavity Surface-Emitting Laser," *IEEE Photon. Technol. Lett.* **22**(14), 1021–1023 (2010).
21. A. H. Quarterman, A. Perevedentsev, K. G. Wilcox, V. Apostolopoulos, H. E. Beere, I. Farrer, D. A. Ritchie, and A. C. Tropper, "Passively harmonically mode-locked vertical-external-cavity surface-emitting laser emitting 1.1 ps pulses at 147 GHz repetition rate," *Appl. Phys. Lett.* **97**(25), 251101 (2010).
22. M. Hoffmann, O. D. Sieber, D. J. H. C. Maas, V. J. Wittwer, M. Golling, T. Südmeyer, and U. Keller, "Experimental verification of soliton-like pulse-shaping mechanisms in passively mode-locked VECSELs," *Opt. Express* **18**(10), 10143–10153 (2010).
23. P. Klopp, U. Griebner, M. Zorn, and M. Weyers, "Pulse repetition rate up to 92 GHz or pulse duration shorter than 110 fs from a mode-locked semiconductor disk laser," *Appl. Phys. Lett.* **98**(7), 071103 (2011).
24. M. Hoffmann, O. D. Sieber, V. J. Wittwer, I. L. Krestnikov, D. A. Livshits, Y. Barbarin, T. Südmeyer, and U. Keller, "Femtosecond high-power quantum dot vertical external cavity surface emitting laser," *Opt. Express* **19**(9), 8108–8116 (2011).
25. K. G. Wilcox, A. H. Quarterman, V. Apostolopoulos, H. E. Beere, I. Farrer, D. A. Ritchie, and A. C. Tropper, "175 GHz, 400-fs-pulse harmonically mode-locked surface emitting semiconductor laser," *Opt. Express* **20**(7), 7040–7045 (2012).
26. M. Scheller, T. L. Wang, B. Kunert, W. Stolz, S. W. Koch, and J. V. Moloney, "Passively modelocked VECSEL emitting 682 fs pulses with 5.1 W of average output power," *Electron. Lett.* **48**(10), 588–589 (2012).
27. C. A. Zaug, M. Hoffmann, W. P. Pallmann, V. J. Wittwer, O. D. Sieber, M. Mangold, M. Golling, K. J. Weingarten, B. W. Tilma, T. Südmeyer, and U. Keller, "Low repetition rate SESAM modelocked VECSEL using an extendable active multipass-cavity approach," *Opt. Express* **20**(25), 27915–27921 (2012).
28. O. D. Sieber, M. Hoffmann, V. J. Wittwer, M. Mangold, M. Golling, B. W. Tilma, T. Südmeyer, and U. Keller, "Experimentally verified pulse formation model for high-power femtosecond VECSELs," *Appl. Phys. B* **113**(1), 133–145 (2013).
29. M. Butkus, E. A. Viktorov, T. Erneux, C. J. Hamilton, G. Maker, G. P. A. Malcolm, and E. U. Rafailov, "85.7 MHz repetition rate mode-locked semiconductor disk laser: fundamental and soliton bound states," *Opt. Express* **21**(21), 25526–25531 (2013).
30. C. A. Zaug, A. Klenner, M. Mangold, A. S. Mayer, S. M. Link, F. Emaury, M. Golling, E. Gini, C. J. Saraceno, B. W. Tilma, and U. Keller, "Gigahertz self-referenceable frequency comb from a semiconductor disk laser," *Opt. Express* **22**(13), 16445–16455 (2014).

31. D. J. H. C. Maas, A.-R. Bellancourt, B. Rudin, M. Golling, H. J. Unold, T. Südmeier, and U. Keller, "Vertical integration of ultrafast semiconductor lasers," *Appl. Phys. B* **88**(4), 493–497 (2007).
32. M. Mangold, V. J. Wittwer, C. A. Zaugg, S. M. Link, M. Golling, B. W. Tilma, and U. Keller, "Femtosecond pulses from a modelocked integrated external-cavity surface emitting laser (MIXSEL)," *Opt. Express* **21**(21), 24904–24911 (2013).
33. C. A. Zaugg, Z. Sun, V. J. Wittwer, D. Popa, S. Milana, T. S. Kulmala, R. S. Sundaram, M. Mangold, O. D. Sieber, M. Golling, Y. Lee, J. H. Ahn, A. C. Ferrari, and U. Keller, "Ultrafast and widely tuneable vertical-external-cavity surface-emitting laser, mode-locked by a graphene-integrated distributed Bragg reflector," *Opt. Express* **21**(25), 31548–31559 (2013).
34. S. Husaini and R. G. Bedford, "Graphene saturable absorber for high power semiconductor disk laser mode-locking," *Appl. Phys. Lett.* **104**(16), 161107 (2014).
35. K. Seger, N. Meiser, S. Y. Choi, B. H. Jung, D.-I. Yeom, F. Rotermund, O. Okhotnikov, F. Laurell, and V. Pasiskevicius, "Carbon nanotube mode-locked optically-pumped semiconductor disk laser," *Opt. Express* **21**(15), 17806–17813 (2013).
36. Y. F. Chen, Y. C. Lee, H. C. Liang, K. Y. Lin, K. W. Su, and K. F. Huang, "Femtosecond high-power spontaneous mode-locked operation in vertical-external cavity surface-emitting laser with gigahertz oscillation," *Opt. Lett.* **36**(23), 4581–4583 (2011).
37. L. Kornaszewski, G. Maker, G. P. A. Malcolm, M. Butkus, E. U. Rafailov, and C. J. Hamilton, "SESAM-free mode-locked semiconductor disk laser," *Laser Photonics Rev.* **6**(6), L20–L23 (2012).
38. A. R. Albrecht, Y. Wang, M. Ghasemkhani, D. V. Seletskiy, J. G. Cederberg, and M. Sheik-Bahae, "Exploring ultrafast negative Kerr effect for mode-locking vertical external-cavity surface-emitting lasers," *Opt. Express* **21**(23), 28801–28808 (2013).
39. M. Gaafar, C. Möller, M. Wichmann, B. Heinen, B. Kunert, A. Rahimi-Iman, W. Stolz, and M. Koch, "Harmonic self-mode-locking of optically pumped semiconductor disc laser," *Electron. Lett.* **50**(7), 542–543 (2014).
40. M. Gaafar, D. A. Nakdali, C. Möller, K. A. Fedorova, M. Wichmann, M. K. Shakfa, F. Zhang, A. Rahimi-Iman, E. U. Rafailov, and M. Koch, "Self-mode-locked quantum-dot vertical-external-cavity surface-emitting laser," *Opt. Lett.* **39**(15), 4623–4626 (2014).
41. H. C. Liang, C. H. Tsou, Y. C. Lee, K. F. Huang, and Y. F. Chen, "Observation of self-mode-locking assisted by high-order transverse modes in optically pumped semiconductor lasers," *Laser Phys. Lett.* **11**(10), 105803 (2014).
42. K. G. Wilcox and A. C. Tropper, "Comment on SESAM-free mode-locked semiconductor disk laser," *Laser Photonics Rev.* **7**(3), 422–423 (2013).
43. L. Kornaszewski, G. Maker, G. P. A. Malcolm, M. Butkus, E. U. Rafailov, and C. J. Hamilton, "Reply to comment on SESAM-free mode-locked semiconductor disk laser," *Laser Photonics Rev.* **7**(4), 555–556 (2013).
44. A. Weiner, *Ultrafast Optics* (Wiley, 2009).

## 1. The path to self-mode-locking

Semiconductor disk lasers (SDLs), also known as vertical-external-cavity surface-emitting lasers (VECSELs), are versatile lasers which serve as an excellent platform for the realization of various emission schemes. The first of its kind was demonstrated in 1997 by Kuznetsov *et al.* [1] and thereafter - owing to their remarkable design flexibility and features - rise was given to a plethora of modifications and improvements towards more specific applications. In recent years, not only high-power multi-mode [2] or single-frequency [3] continuous-wave operation schemes have been achieved, but also two-color [4] as well as mode-locked [5] emission. Particularly, their external resonator is predestined to be exploited for intra-cavity frequency conversion via nonlinear elements which expands the accessible wavelength range drastically. While second-harmonic generation pushes the boundaries into the UV [6], even terahertz frequencies can be reached using difference-frequency generation inside a two-color VECSEL [7, 8] - to name a few remarkable achievements in this field.

Within the last decade, VECSELs have become particularly appealing sources of pulsed laser light, because they can typically provide a high output power and an outstanding beam quality. The demonstration of the first mode-locked (ML) VECSEL dates back to the year 2000 and was achieved by Hoogland *et al.* for a central wavelength of 1  $\mu\text{m}$  with 22 ps long pulses [9]. It did not take long and VECSELs were considered becoming compact, cost-efficient alternatives to commercial mode-locked lasers with ever shorter pulses, higher peak powers and enhanced tunability using resonator-integrated [10–30] or even chip-integrated [31, 32] semiconductor saturable-absorber mirrors (SESAMs). However, the complex, power-sensitive and costly SESAMs, which have to be carefully designed for a certain wavelength

range, naturally impose limitations on the performance of the device. Currently, besides semiconductor materials, graphene [33, 34] as well as carbon nanotubes [35] saturable absorbers have been employed for ML operation of VECSELs. However, mode-locking has also been reported to take place even without any additional saturable absorber—an effect called self-mode locking (SML) [36–41].

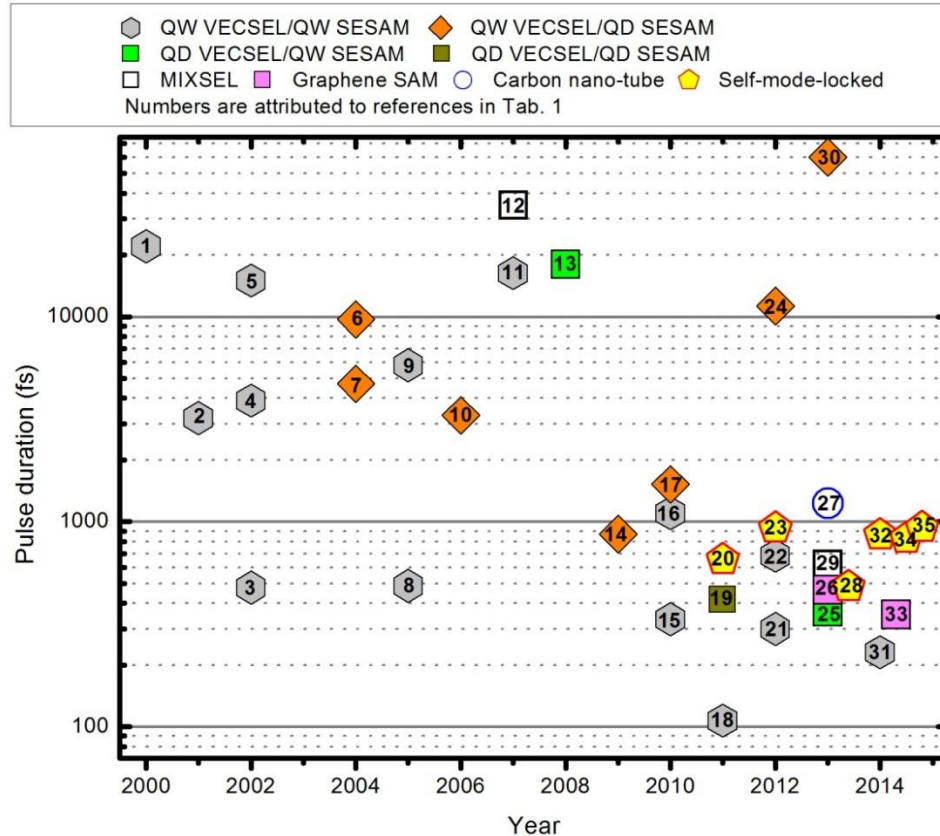


Fig. 1. Overview of pulse durations of mode-locked optically pumped VECSELs emitting around 1  $\mu\text{m}$  wavelength. More details including references are presented in Table 1.

In this work, light is shed on recent demonstrations of SESAM-free VECSELs which are operated under SML conditions. It was recently demonstrated that the SML scheme is not only applicable to quantum-well VECSELs [36–39, 41], but also to quantum-dot devices [40]. Furthermore, SML can be used for passively harmonically mode-locked devices with sub-ps-pulsed operation demonstrated at discrete power levels up to the third harmonic [39]. Inherently, this novel and effective technique allows for a maximum degree of wavelength flexibility and a reduction of device complexity. However, the mechanism of SML, which could give access to an exhaustive utilization of the occurring effects, is not fully understood yet and will be subject to future studies - noting that different driving mechanisms for SML were proposed [36–38, 41]. Nevertheless, an optimization of the dispersion management as well as the thermal management in an optimistic view promises the achievement of shorter pulses in the sub-100-fs range and significantly higher peak powers exceeding the current values at repetition rates ranging from a few hundreds of MHz to a few GHz.

In Fig. 1, an overview of all mode-locking techniques of optically pumped VECSELs around a wavelength of 1  $\mu\text{m}$  is shown. More details and the attribution of numbers to references can be found in Table 1.

**Table 1. Overview of fundamentally mode-locked optically pumped VECSELs emitting around 1  $\mu\text{m}$  wavelength**

Number in Fig. 1	Year	Type	Pulse duration	Repetition rate (GHz)	Average output power (W)	Reference
1	2000	QW-VECSEL/QW-SESAM	22 ps	4.4	0.022	[9]
2	2001	QW-VECSEL/QW-SESAM	3.2 ps	2.06	0.213	[10]
3	2002	QW-VECSEL/QW-SESAM	477 fs	1.21	0.1	[11]
4	2002	QW-VECSEL/QW-SESAM	3.9 ps	5.95	0.53	[12]
5	2002	QW-VECSEL/QW-SESAM	15 ps	6	0.95	[12]
6	2004	QW-VECSEL/QD-SESAM	4.7 ps	30	0.025	[13]
7	2004	QW-VECSEL/QD-SESAM	9.7 ps	21	0.055	[13]
8	2005	QW-VECSEL/QW-SESAM	486 fs	10.01	0.0303	[14]
9	2005	QW-VECSEL/QW-SESAM	5.8 ps	1.88	0.083	[15]
10	2006	QW-VECSEL/QD-SESAM	3.3 ps	50	0.1	[16]
11	2007	QW-VECSEL/QW-SESAM	16.3 ps	0.35	0.013	[17]
12	2007	MIXSEL	35 ps	2.8	0.04	[31]
13	2008	QD-VECSEL/QW-SESAM	18 ps	2.57	0.027	[18]
14	2009	QW-VECSEL/QD-SESAM	870 fs	0.9	0.045	[19]
15	2010	QW-VECSEL/QW-SESAM	335 fs	1	0.12	[20]
16	2010	QW-VECSEL/QW-SESAM	1.1 ps	147	0.04	[21]
17	2010	QW-VECSEL/QD-SESAM	1.52 ps	4.2	0.03	[22]
18	2011	QW-VECSEL/QW-SESAM	107 fs	5.14	0.003	[23]
19	2011	QD-VECSEL/QD-SESAM	416 fs	4.5	0.143	[24]
20	2011	QW-self-mode-locking	654 fs	2.17	0.45	[36]
21	2012	QW-VECSEL/QW-SESAM	300 fs	169	0.02	[25]
22	2012	QW-VECSEL/QW-SESAM	682 fs	1.71	5.1	[26]
23	2012	QW-self-mode-locking	930 fs	0.21	1.5	[37]
24	2012	QW-VECSEL/QD-SESAM	11.3 ps	0.253	0.4	[27]
25	2013	QD-VECSEL/QW-SESAM	364 fs	3.97	0.07	[28]
26	2013	Graphene SAM	466 fs	2.48	0.013	[33]
27	2013	Carbon nano-tube	1.23 ps	0.613	0.136	[35]
28	2013	QW-self-mode-locking	482 fs	1	1	[38]
29	2013	MIXSEL	620 fs	4.8	0.101	[32]
30	2013	QW-VECSEL/QD-SESAM	60 ps	0.085	0.36	[29]
31	2014	QW-VECSEL/QW-SESAM	231 fs	1.75	0.1	[30]
32	2014	QW-self-mode-locking	860 fs	0.504	0.47	[39]
33	2014	Graphene SAM	353 fs	1.76	10.2	[34]
34	2014	QD-self-mode-locking	900 fs	1.5	0.75	[40]
35	2014	QW-self-mode-locking	935 fs	1.8	—	[41]

Yet, the mode-locking semiconductor-laser community doubts that previous publications about SML truly show mode-locked devices. In our work, we intend to address concerns that have been discussed recently. Most prominent is the discussion presented in Refs [42, 43] triggered by a report on SESAM-free ML-VECSEL [37]. In the following, we provide clear evidence of SML by a variety of measurements: Green light originating from second-harmonic generation using the out-coupled laser beam is observed when our device is running in the ML regime. Furthermore, by presenting long-time-span pulse trains as well as radiofrequency-spectra measurements for our sub-ps pulses at 500 MHz repetition rate we highlight the stability of our device. In addition, a long-time-span autocorrelation trace shows absence of a pedestal or double pulses. Finally, we show a beam-profile measurement which reveals the excellent beam quality of our device with an M-square factor of less than 1.1 for both axes.

## 2. VECSEL chip design and setups

The VECSEL chip used in our experiments is grown by metal-organic-vapour-phase-epitaxy. The gain medium consists of 10 (InGa)As quantum wells (QWs) equally spaced by  $\lambda/2$  GaAsP barrier layers.  $24\frac{1}{2}$  pairs of quarter wavelength GaAs/AlGaAs layers form a distributed Bragg reflector (DBR). Both, QWs and DBR are designed for a laser emission at approximately 1010 nm. The semiconductor structure is flip-chip-bonded using Au-In solid-liquid inter-diffusion bonding onto a 350  $\mu\text{m}$  thick CVD-diamond heat spreader before wet etching to remove the substrate.

An anti-resonant micro-cavity design is chosen in order to minimize the group delay dispersion (GDD) and to spectrally broaden the effective gain of the structure. Therefore, the (InGa)P cap layer is etched down to a thickness of  $1.25\lambda/4$ , which theoretically results in a negligible GDD at the design wavelength. The electric-field (E-field) distribution inside the gain medium is shown in Fig. 2(a). The positions of the quantum wells are represented by the vertical red lines. The laser setup is schematically shown in Fig. 2(b): The cavity is optimized for mode-locked operation assuming Kerr-lensing inside the VECSEL chip structure [38]. Therefore, a variable slit is placed directly in front of a highly reflective end mirror (HR). The Z-shaped cavity consists of a flat output coupler (OC) with a transmittance of 1.6%, the gain chip itself, and a highly reflective curved mirror (CM) with a radius of curvature of 150 mm as well as the HR mirror. With a total cavity length amounting to 30 cm a free spectral range of approximately 0.5 GHz is determined. The laser chip is mounted onto a water-cooled copper heat sink and pumped under an incident angle of  $30^\circ$  using an 808 nm fiber-coupled diode laser which is focused onto the chip and ensures a pump mode of adjustable size. The angle of incidence on the curved mirror was kept below  $10^\circ$  in order to avoid excessive astigmatism.

## 3. Evidence of self-mode-locked operation

In our VECSEL, mode-locking is initiated when the slit in front of the HR end mirror is moved or the slit width is narrowed. Furthermore, the cavity length was fine-tuned to stabilize SML operation (cf [39, 40]). In order to clearly demonstrate mode-locked operation employing the SML technique, different measurements have to be carried out [42]. Usually radiofrequency (RF) spectra, optical spectra, autocorrelation traces are sufficient for the characterization of mode-locking operation. However, if a new mode-locking technique is introduced, further measurements are required in order to exclude artificial effects and the standard characterization methods cannot serve as an unambiguous evidence of mode-locking. One of these artificial effects that could give the impression of a ML device is mode-beating which could result in an RF spectrum similar to which is recorded with a ML device. This was clearly demonstrated in [42]. Moreover, an autocorrelation trace can also be misleading as a CW signal may result in a time trace which gives rather information about the coherence length than about a pulse duration [44]. The possibility that both RF spectra and autocorrelation traces, which are presented in the next section, are misapprehended can be banned by recording externally the second-harmonic generation (SHG) signal of our SML-VECSEL.



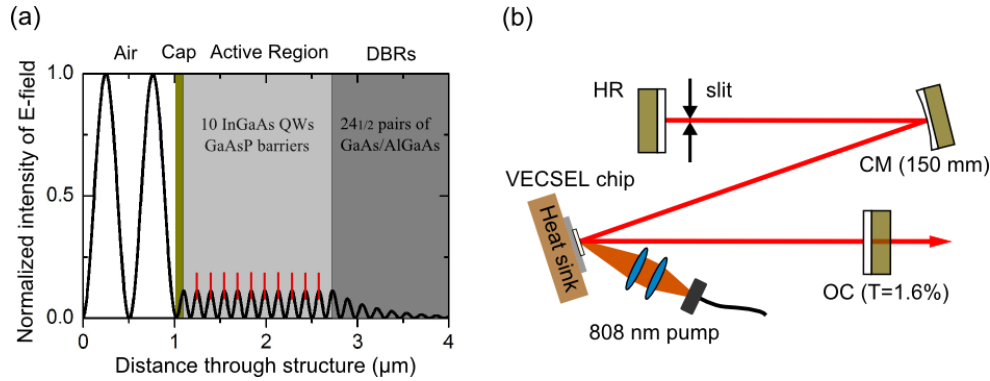


Fig. 2. (a) E-field distribution inside the near-antiresonant gain structure, normalized to the input intensity. The positions of the quantum wells are represented by the vertical red lines. (b) Schematic drawing of the setup of SML optically pumped VECSEL.

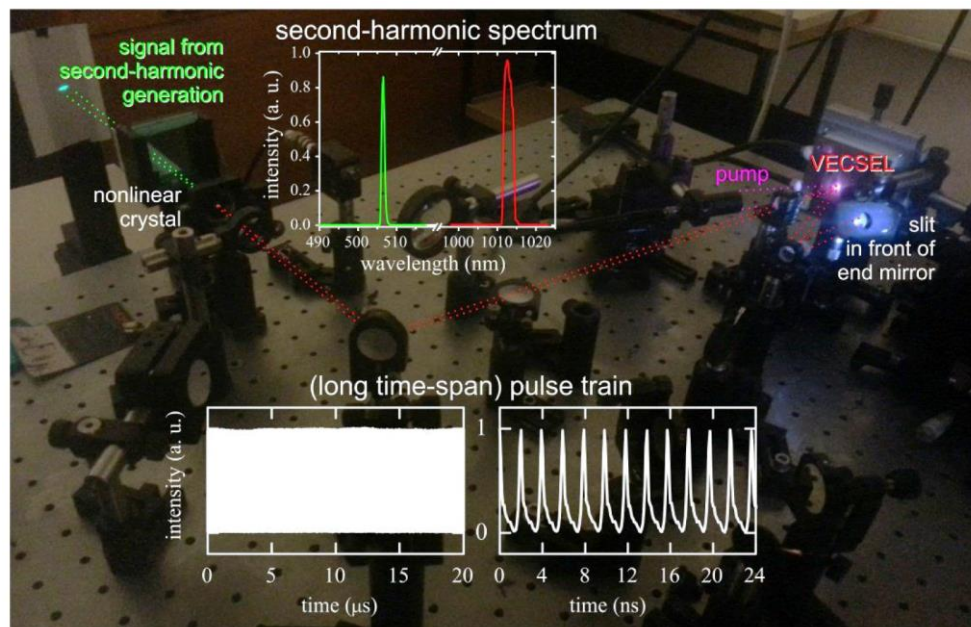


Fig. 3. Self-mode-locked quantum-well semiconductor disk laser: Green light is externally produced via second-harmonic generation with the infrared pulsed laser light. Inset: The spectrum shows the frequency-doubled signal originating from SHG using the out-coupled VECSEL beam (top). The diagram of the long-span pulse train of this device is shown at the bottom (left). The close-up of the pulse train reveals a 500-MHz repetition rate for the fundamental mode (right).

A nonlinear frequency conversion in a BBO crystal is performed using an SML VECSEL for the first time, to the best of our knowledge. Therefore, the out-coupled laser beam of the VECSEL is directed into the nonlinear crystal, as seen in Fig. 3, so that green light is externally produced via SHG with the infrared pulsed laser light. In case of continuous-wave operation no SHG signal is observed whereas a clear spectrum of the SHG signal can be measured if the laser is mode-locked, since SHG is an intensity-dependent nonlinear effect. The top inset of Fig. 3 shows the corresponding spectrum of the frequency-doubled signal (507 nm) originating from SHG using the out-coupled SML VECSEL beam (1013 nm). The photo shown in Fig. 3 presents the actual setup used for this experiment with colored dotted lines indicating the beam path inside and outside the VECSEL. The slit is highlighted by flash

light and is placed directly in front of the HR mirror of the cavity. A lens is used to focus the VECSEL output into the nonlinear crystal, as shown in the left part of the photo.

To highlight stable mode-locked operation of our QW VECSEL, a representative long-span pulse-train of the output is shown as inset on the bottom of Fig. 3. The signal was recorded for both a time window of 20  $\mu$ s (bottom-left) and a few ns (bottom-right), respectively, via an InGaAs photodetector (PD) with a 3 dB bandwidth of 5 GHz and a digital oscilloscope with an analog bandwidth of 2 GHz. Stable mode-locking can be derived from this measurement as the pulse train with approximately 500 MHz repetition rate exhibits no intensity modulations.

#### 4. Characterization of the emission features

In this section, we present RF-spectra measurements as well as time-resolved autocorrelation data of a VECSEL operated under SML conditions. Moreover, a beam-profile measurement is performed in order to reveal the excellent beam-quality of our device. Since RF-spectra measurements provide information on the frequency stability of the generated pulses, measurements are performed with a 3-dB bandwidth of a 5-GHz PD coupled to a 22-GHz-bandwidth electrical spectrum analyzer (HP 8566A). Figure 4 shows the RF spectrum of the fundamental repetition rate measured using a 10 kHz resolution bandwidth (RBW). Here, a clear peak at 504 MHz with a signal to noise ratio of about 50 dB is observed. The RF linewidth is less than 30 kHz, which highlights the stable operation of our mode-locked system. This result is similar to those obtained from SESEAM mode-locked VECSELs [12, 27]. The inset of Fig. 4 presents the RF spectrum of the first 9 harmonics indicating a stable pulse generation with no parasitic sidebands around the fundamental and higher harmonics frequencies.

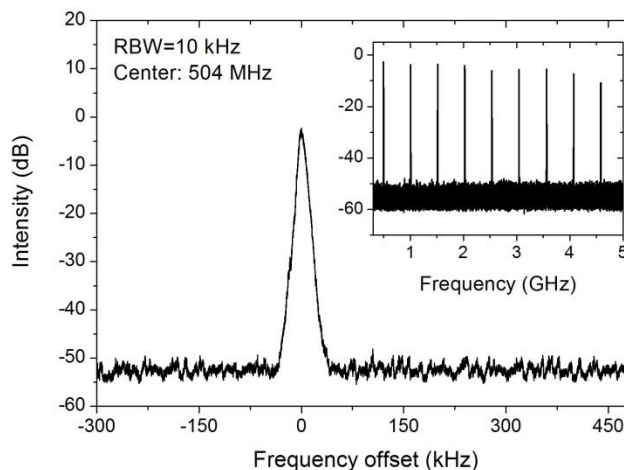


Fig. 4. RF spectrum of the fundamental repetition rate recorded with a 10 kHz resolution bandwidth (RBW). Inset: 5 GHz span showing the first 9 harmonics of the self-mode-locked device.

The mode-locked pulse duration was measured with a self-made intensity autocorrelator with a scan range of  $\sim$ 130 ps. Figure 5(a) shows a long-delay autocorrelation trace for fundamental mode-locking confirming the single-pulse operation. To complement the information, a short-delay autocorrelation trace with  $\text{sech}^2$ -fit is shown in Fig. 5(b) which yields a pulse duration of 860 fs. The corresponding optical spectrum was measured using an Ando AQ-6315A optical spectrum analyzer. The spectrum has a full width at half maximum of 2.7 nm, resulting in a time bandwidth product (TBWP) of 0.68 (Fig. 5(c)). The average



output power was measured to be 460 mW for this QW VECSEL which leads to a peak power of 950 W.

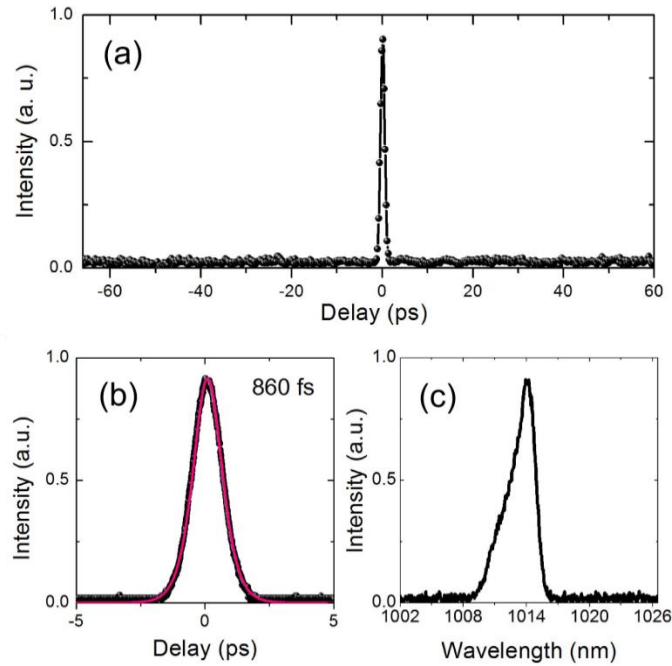


Fig. 5. (a) A long-delay autocorrelation trace for fundamental mode-locking confirming the single pulse operation. (b) A short delay autocorrelation trace with  $\text{sech}^2$ -fit precisely determines the pulse duration of 860 fs. (c) The corresponding optical spectrum centered at 1014 nm.

Finally, the beam quality was measured for an average output power of 450 mW, see Fig. 6: Excellent M-square values of 1.07 and 1.08 in the horizontal and vertical directions respectively have been obtained, confirming lasing in the fundamental transverse mode with nearly ideal Gaussian characteristics. The inset shows a corresponding beam-profile under SML operation. While Liang *et al.* [41] supposed that the occurrence of SML can be assisted by the existence of high-order transverse modes, our results are in contrast to these findings. Liang *et al.* observed a threshold for SML which coincided with the threshold of high-order transverse modes. With our results we rule out a dependence of SML on high-order transverse modes and demonstrate an excellent beam quality of our SML VECSEL with fundamental-transverse-mode profile.

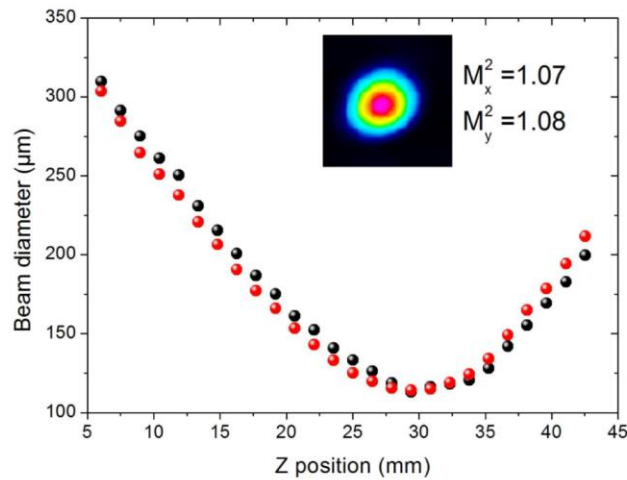


Fig. 6. Beam quality measurement confirming operation in fundamental-transverse mode with  $M^2$  values less than 1.1 for both axes.

## 5. Conclusion

To summarize, we highlighted recent achievements in the field of ML and in particular SML VECSEL and presented a clear evidence of mode-locking for a QW device under SML conditions. Green light originating from second-harmonic generation in an external BBO crystal was demonstrated using the out-coupled laser beam. In addition, long-time-span pulse trains as well as radiofrequency spectra measurements were presented for our sub-ps pulses at 500 MHz repetition rate which indicate the stable pulse operation of our device. Furthermore, a long-time-span autocorrelation trace, which emphasizes the absence of a pedestal or double pulses, was shown. Additionally, a beam-profile measurement revealed the excellent beam quality of the device with an M-square factor of less than 1.1 for both axes. Even though the driving mechanism for SML has to be studied with care in future investigation for an efficient use of the underlying effects, we believe that in the near future SML VECSELs, which combine the advantages of solid-state and semiconductor devices, can become robust, compact and low-cost sources of fs-pulsed laser light.

## Acknowledgment

The authors acknowledge financial support from the German Science Foundation (DFG: GRK 1782, SFB 1083). M. Gaafar acknowledges support from the Yousef Jameel scholarship funds. H. Keskin acknowledges financial support from COST Action MP1204 as well as The Scientific and Technical Research Council of Turkey under grant #111T748 via H. Altan. The authors would like to thank E. U. Rafailov, K. A. Fedorova and A. A. Gorodetsky for fruitful discussions and G. Bastian for providing the fast oscilloscope. The authors further would like to thank B. Heinen and B. Kunert for VECSEL-chip processing.